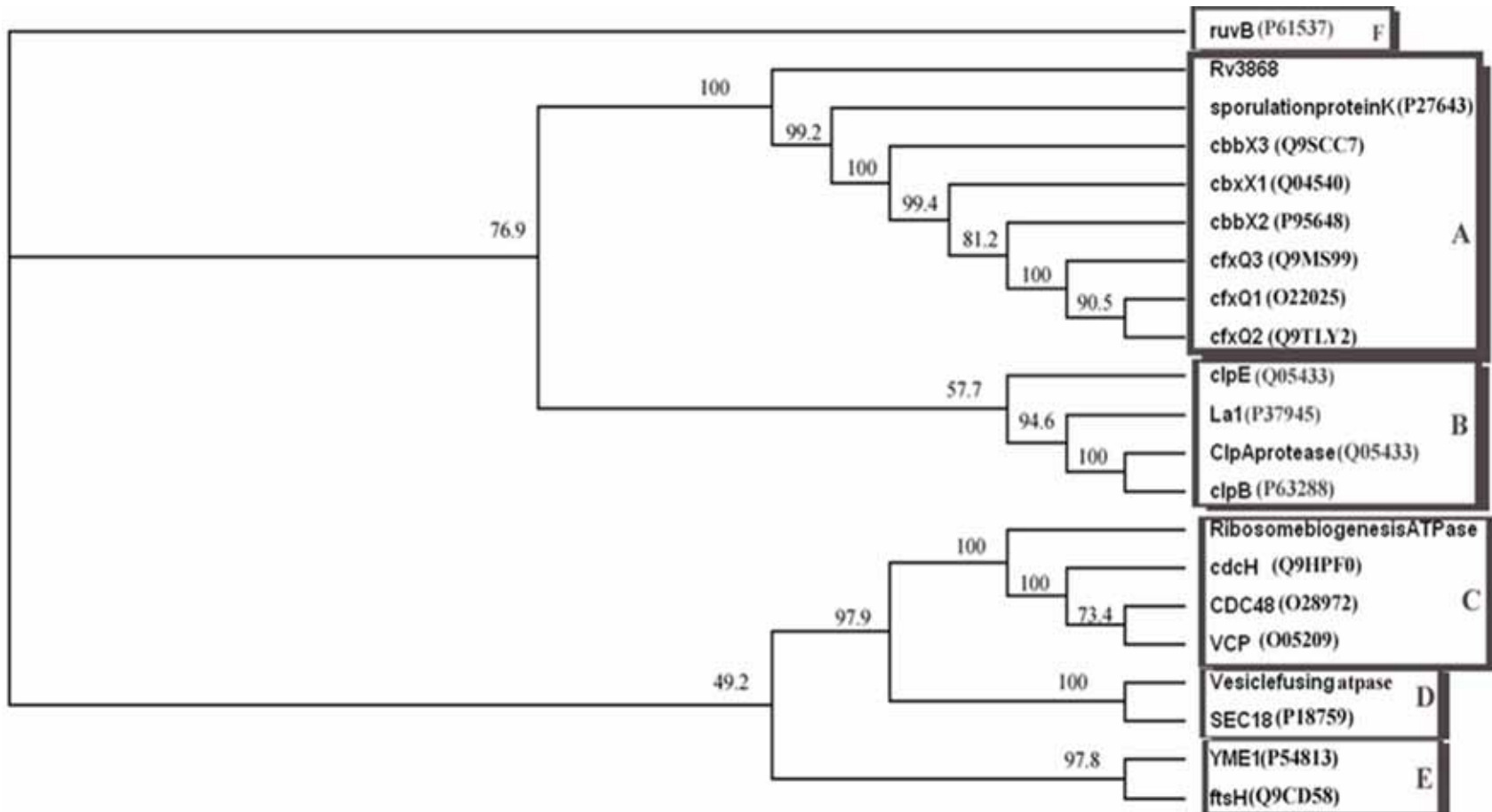


SUPPLEMENTARY INFORMATION
(Luthra & Ramachandran, 2008)

Supplementary Table 1:

Primers used for the cloning of Rv3868, CT-Rv3868 and its mutants

Primer Name	Primer sequence
Rv3868 Forward	5'-CGGGACCAACATATGACTGATCGCTTAGC-3'
Rv3868 Reverse	5'- TTGAAGCTTTTCTCTCATGTTGAGGTG -3'
CT-Rv3868 Forward	5'-CCAGGATCCATGATCTTCACCGGCC-3'
CT-Rv3868 Reverse	5'-TTGAAGCTTAGCTGCGGCAATGACGTTGGC-3'
P336A sense	5'-TCACCGGACCGGCCGGTACCGGC-3'
P7A antisense	5'-GCCGGTACCGGCCGGTCCGGTGA-3'
T338A sense	5'-CCGGACCGCCCGGTGCCGGCAAG-3'
T338A antisense	5'-CTTGCCGGCACCGGGCGGTCCGG-3'
K340A sense	5'-GCCCCGGTACCGGCGCGACCACGATCGCG-3'
K340A antisense	5'-CGCGATCGTGGTCGCGCCGGTACCGGGC-3'
R429A sense	5'-GATGGAGAACGACGCGGACCGGCTGGTG-3'
R429A antisense	5'-CACCAGCCGGTCCGCGTCGTTCTCCATC-3'
Y439A sense	5'-GTGATCATCGCCGGGGCCAGCTCCGACATAGAT-3'
Y439A antisense	5'-TCTATGTTCGGAGCTGGCCCCGGCGATGATCACC-3'
Y466A	5'-CATCGAGTTCGACACCGCTTCCCCGAGGAACTC-3'
Y466A antisense	5'-GAGTTCCTCGGGGGAAGCGGTGTCGAACTCGATG-3'

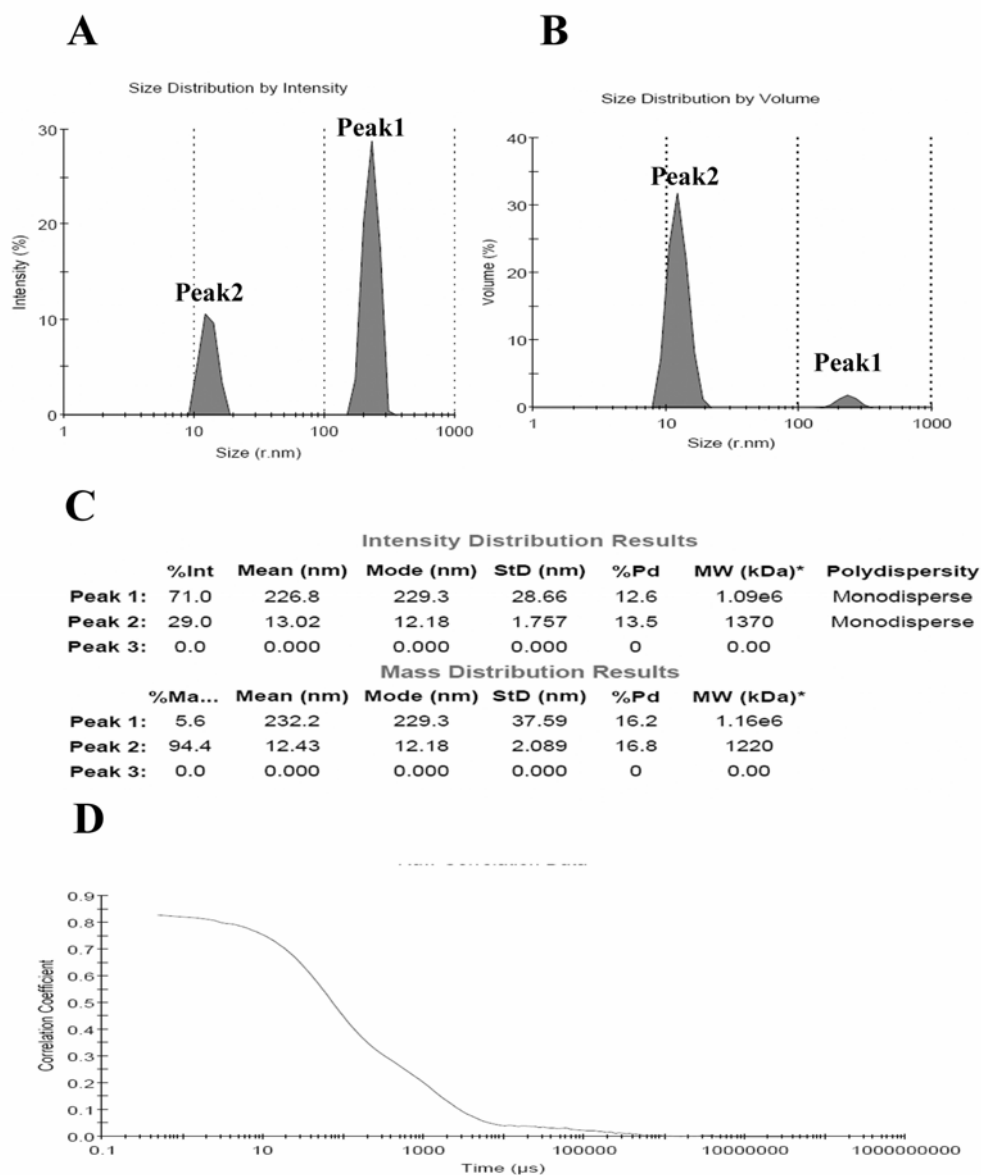


Supplementary Figure 1: Evolutionary analysis of Rv3868

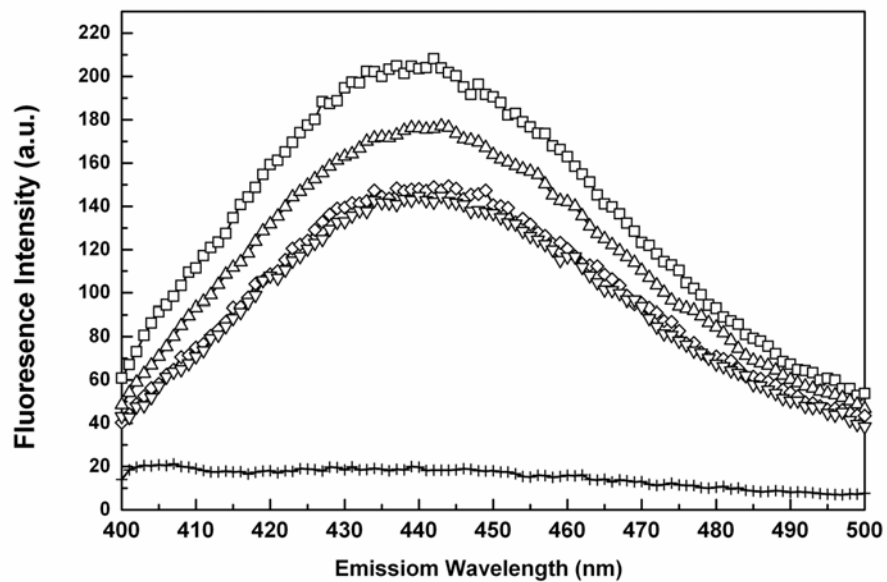
Phylogenetic tree calculated for different AAA-ATPase protein families with the major proteins highlighted in boxes:

A, CbbxX family; **B**, Periplasmic chaperones ; **C&D**, Cdc/p97; **E**, Metallopeptidases; **F**, DNA helicases

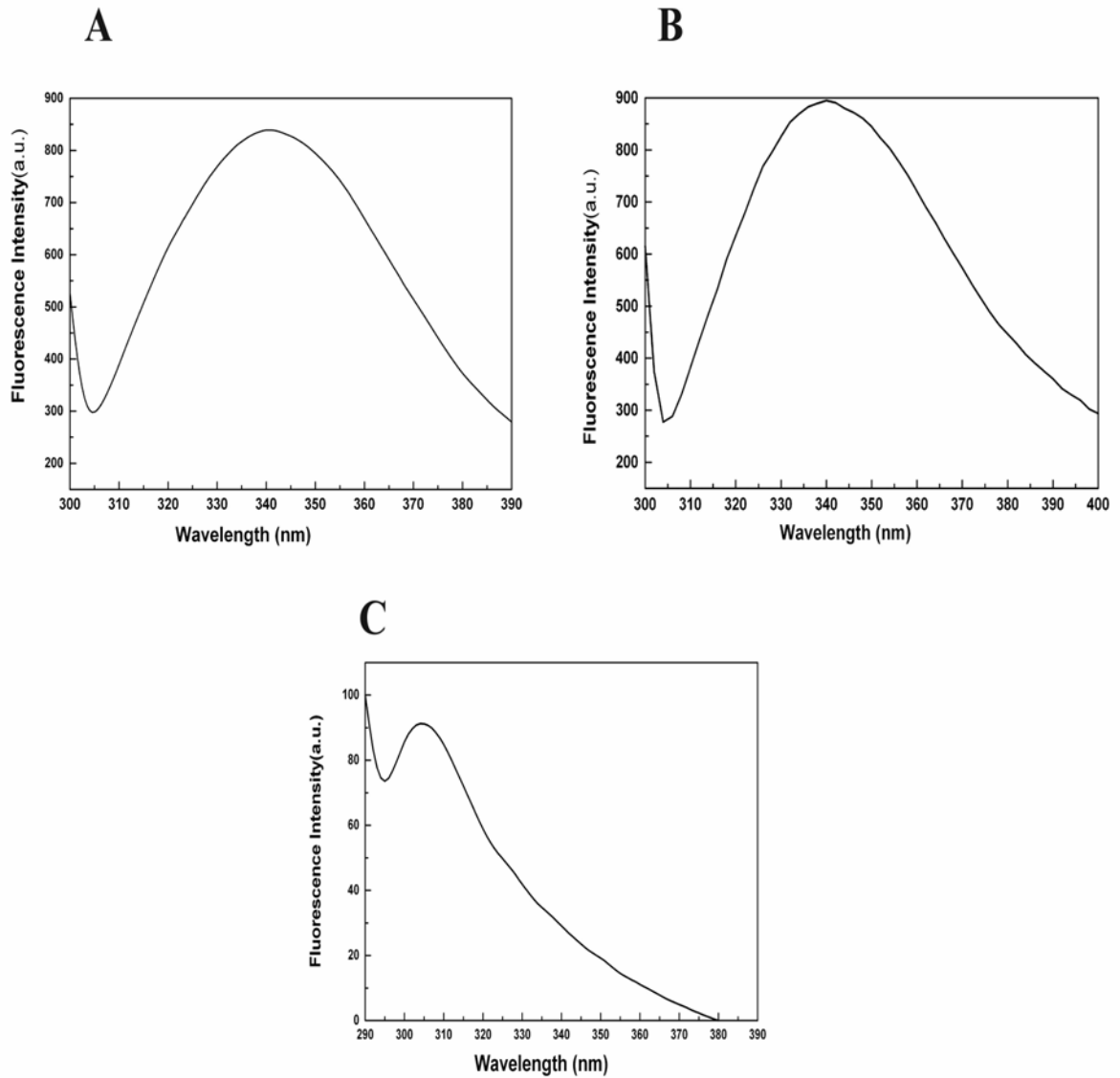
The *Swiss-Prot* No. is given in brackets. Bootstrap values (%) are indicated for the major branch points in the tree. To generate the family relationships shown in the tree, the protein sequences were aligned initially and then bootstrapped 1,000 times using the PAM 250 amino acid comparison table.



Supplementary Figure 3: Dynamic light scattering experiments involving Rv3868
 Size distribution based on
 (A) Intensity and (B) Volume studied by DLS for a solution containing ~10 μ M Rv3868 in 25 mM Tris, pH 7.5 & 50mM NaCl.
 (C) Analysis of molecular weight and monodispersity of higher order oligomers (peak2) and aggregates (peak1). Polydispersity (Pd) <20% of the sample indicates the absence of non-specific aggregates.
 (D) A plot of the correlation coefficient with respect to time (μ s) also shows a bimodal size distribution for the sample suggesting two populations of different oligomeric states.

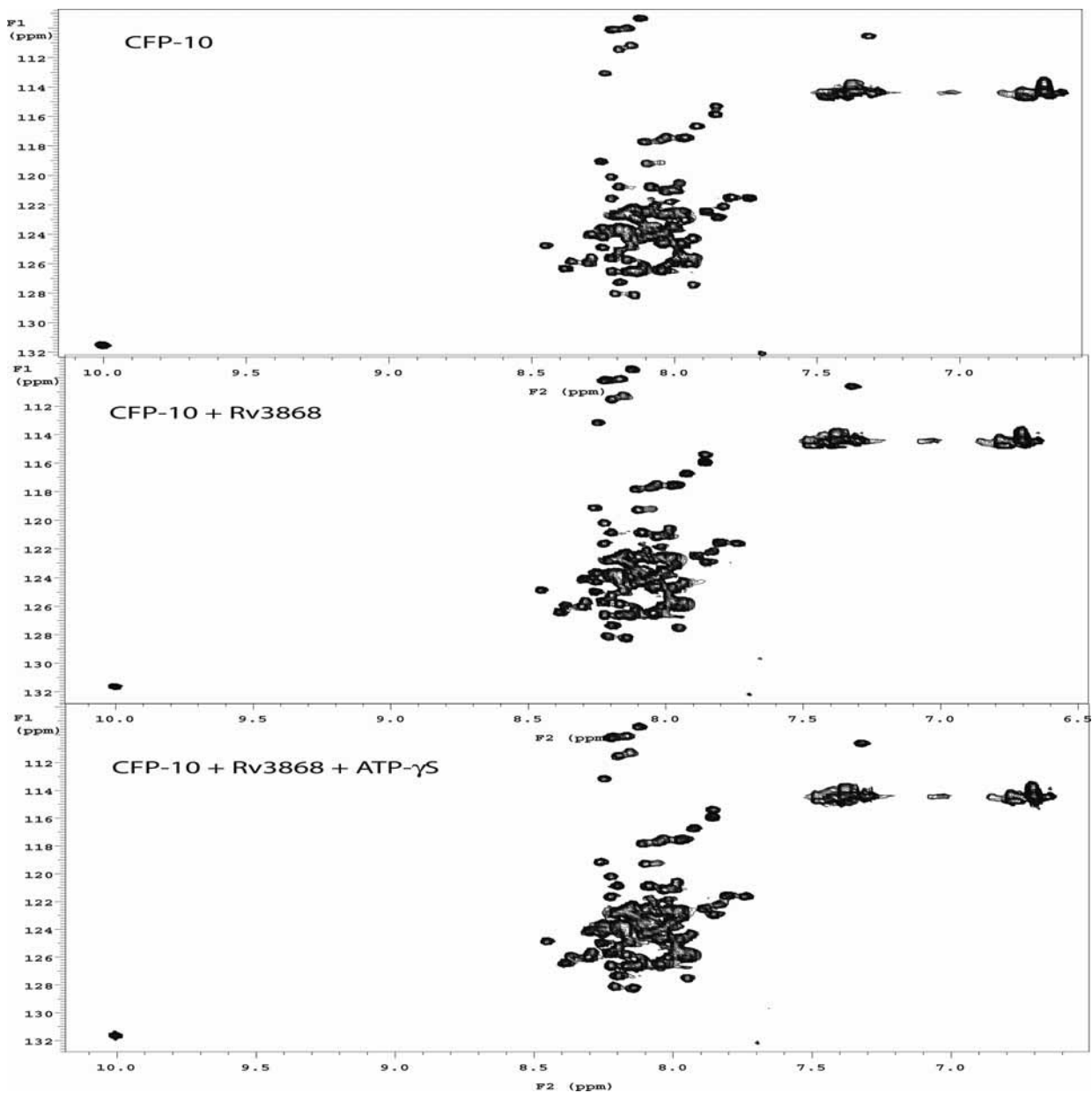


Supplementary Figure 4: Qualitative study of the binding of MANT-ATP to CT-Rv3868 studied by fluorescence spectroscopy. Fluorescence emission spectra of 1.0 μ M CT-Rv3868 in the absence of MANT-ATP (-|-|-), 1 μ M MANT-ATP in the absence of protein (\square) and in the presence of 0.5 μ M of CT-Rv3868 (Δ) and 1.0 μ M of CT-Rv3868 (\diamond).



Supplementary Figure 5: Fluorescence emission spectra of: (A) Rv3868, (B) NT-Rv3868 & (C) CT-Rv3868

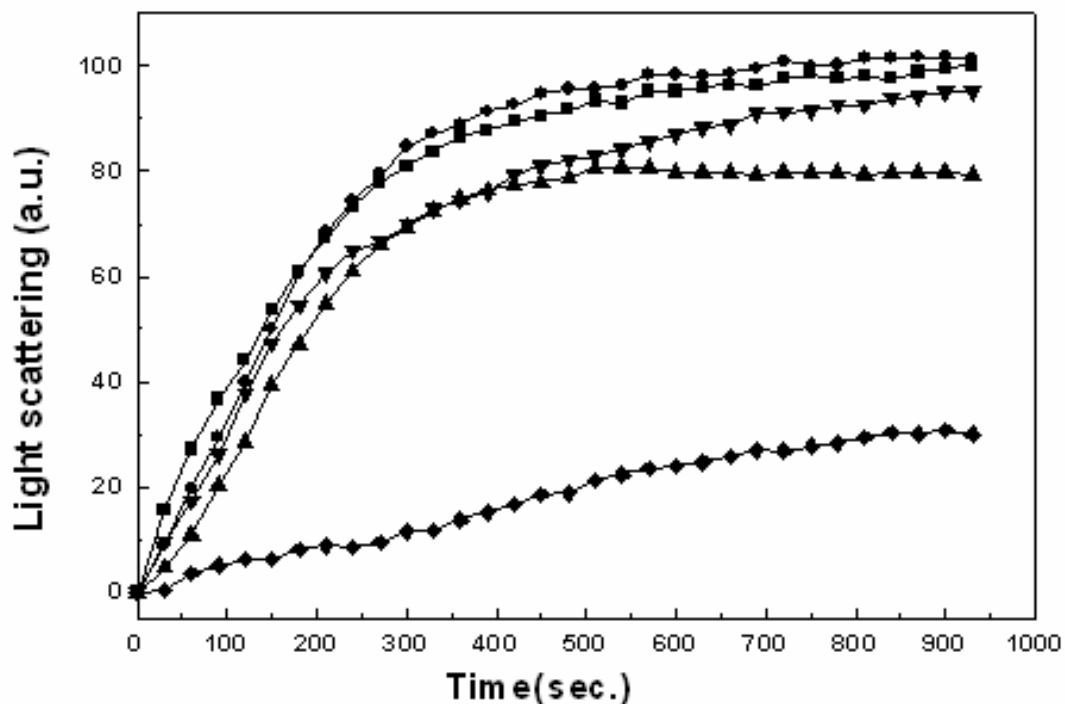
All Trp residues are present only in NT-Rv3868. The C-terminal domain does not contain Trp residues. The samples were in 25mM Tris, pH 7.5, 50mM NaCl



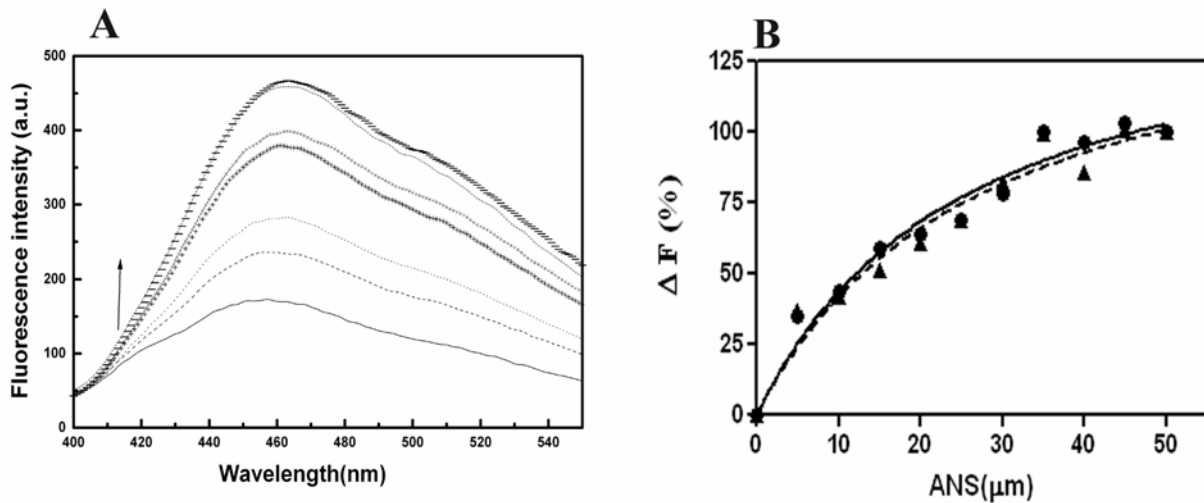
Supplementary Figure 6: HSQC spectra of CFP-10

(A) [^{15}N - ^1H] HSQC spectra of ^{15}N -labeled CFP-10 in Free State. (B) [^{15}N - ^1H] HSQC spectra of ^{15}N -labeled CFP-10 in presence of unlabeled Rv3868. (C) ^{15}N -labeled CFP-10+Rv3868+ATP- γ S.

The three spectra are nearly identical and indicate no change in the conformation of CFP-10 in the presence of Rv3868 with/without added nucleotide. This is unlike its interactions with ESAT-6 (See Ref. 11 in the paper) where it was observed that complex formation leads to large structural changes in the protein.



Supplementary Figure 7: Possible chaperone functions were probed by following the thermal aggregation of lysozyme in the presence and absence of Rv3868. The thermal aggregation of lysozyme is not inhibited by Rv3868 in a concentration-dependent way. The aggregation of lysozyme was followed by light scattering at 360 nm in a Perkin-Elmer lambda 25 spectrophotometer with a Peltier system. (A) Temperature (45 °C) induced aggregation of lysozyme in the absence (▲) and at increasing molar ratios of lysozyme: Rv3868 of 1:5 (▼); 1:10 (■), and 1:10+ATP (●) respectively were followed. The control experiments involved following the scattering by Rv3868 (◆) alone.



Supplementary Figure 8: Study of ANS binding to Rv3868 and its variants by fluorescence spectroscopy (**A**) The fluorescence intensity of ANS is enhanced upon binding to Rv3868. Its fluorescence is also observed to increase significantly in the presence of both Rv3868 (**A**) and CT-Rv3868 (*not shown*). The direction of the arrow represents the enhancement seen in the presence of ANS (**B**) The relative change (%) in fluorescence intensity at 470 nm plotted against the ANS concentration in experiments involving Rv3868 (\blacktriangle) and CT-Rv3868 (\bullet) respectively.